Chaotic Dynamics of a Piecewise Smooth Overlapping Generations Model with a Multitude of Technologies

Yosuke Umezuki [*] and Masanori Yokoo [†]

This Version: January 31, 2019

Abstract

In this study, we develop a simple overlapping generations model that can exhibit chaotic fluctuation. The key assumption is that a firm's owner can choose from a continuum of technologies of production. As a result, the model reduces to a piecewise smooth map, which is tractable enough so its dynamics can be analytically investigated in depth. To study chaotic behaviors in the model, we adopt two approaches: *border collision bifurcation* and *Markov property*. The border collision bifurcation theory characterizes the routes from a globally attracting steady state to other non-stationary behaviors. The Markov property reveals the chaotic dynamics of the model for a much larger set of parameter values.

---

[*]Corresponding author: Graduate School of Humanities and Social Sciences, Okayama University, Tsushimanaka 3-1-1, Kita-ku, Okayama 700-8530, Japan. e-mail: ec19025@s.okayama-u.ac.jp

[†]Graduate School of Humanities and Social Sciences and Faculty of Economics, Okayama University, Tsushimanaka 3-1-1, Kita-ku, Okayama 700-8530, Japan. e-mail: yokoo@e.okayama-u.ac.jp

1 Introduction

There is no doubt that the overlapping generations (OLG, hereafter) model is one of the most popular dynamic economic models in the literature. Especially, the OLG setting plays an important role in constructing an endogenous growth (or business) cycle model, which exhibits, without external shocks, a perpetual periodic or chaotic (i.e., random-looking but deterministic) fluctuation. In early literature, a few prominent examples of such perpetual fluctuation in an OLG model can be found in the studies by Benhabib and Day (1982) and Grandmont (1985).

Matsuyama (2007) presents an OLG-type model of credit cycles induced by financial imperfections; he shows that the model has the capability to exhibit several dynamic growth patterns, including perpetual fluctuations. Asano et al. (2012) focus on a special case of the model by Matsuyama (2007) and show that, in such a case, the model can exhibit periodic and non-periodic fluctuations. Iwaisako (2002) investigates a situation in which investors can choose from among two production technologies—constant returns to scale and increasing returns to scale—and shows several dynamic patterns such as perpetual fluctuation and permanent economic growth. It should be noted that, in the above studies, each model can eventually reduce to a one-dimensional map with discontinuity. In these models, the set of parameter values for which a complex fluctuation can appear is extremely "thin" even if there exists a complex fluctuation theoretically. In other words, the chaotic motions cannot be observed virtually.

Along this line of discrete choice in an OLG model, Umezuki and Yokoo (2019) construct an explicit OLG model in which the firm faces a binary choice problem related to the choice of technology (represented by the Cobb-Douglas production function of constant returns to scale). Similar to the above studies, our model can eventually reduce to a piecewise linear map with discontinuity. Such piecewise-linearization, similar to Asano et al. (2012), helps us to directly apply to our model some useful results borrowed from prior studies on mathematical neuron models. The employment of this method completely characterizes the existence and occurrence of periodic fluctuations in the model. However, the model also cannot virtually reproduce complex fluctuations, because it has a small set of parameter values for which there exists non-periodic fluctuation in the model.

Of course, we can frequently observe *non*-periodic, complex fluctuation of economic variables in the real world. Therefore, it is natural that, along this line, we develop a model that can virtually reproduce the chaotic fluctuations in the long run. Especially, this study aims to extend the model in Umezuki and Yokoo (2019). To do this, our idea is to smooth the map with discontinuity through some modifications. If this new piecewise

smooth map has sufficient nonlinearity, we can easily conjecture that the model has the capability to generate observable complex fluctuations.

It must be noted that the approach to smooth the discontinuous model has been discussed in context. Yokoo and Ishida (2008) introduce imperfect observability, which they call misperception. It is represented by a parameterized random variable in the state variable to smooth Ishida and Yokoo's (2004) piecewise linear model with discontinuity, which is a macroeconomic, but not an OLG, model with discrete choice. Asano and Yokoo (2019) also adopt this idea into the model in Asano et al. (2012) and investigate the chaotic dynamics. However, in general, the abovementioned smooth model with imperfect observability is too general to investigate its dynamics in detail. Indeed, these studies make a somewhat strict assumption about misperception, in which the model can reduce to a piecewise *linear* map. Although such linearization gives us depth and clear results about the complex dynamics of the model, there is a tradeoff between tractability and generality in this method.

On the other hand, in this study, we use a more primitive and intuitive way to smooth Umezuki and Yokoo's (2019) piecewise linear map with discontinuity. There is only one modification: we assume that the firm faces a *continuous* choice problem of technology rather than a binary choice problem. As a result, we can transform, without additional assumption, a piecewise linear model with discontinuity into a continuous piecewise smooth model that can virtually reproduce the chaotic motion and is tractable enough to investigate such a fluctuation. In this sense, our model can cope with both generality and tractability. Matsuyama (2013) and Matsuyama et al. (2016) adopt the same method, which assumes a continuous choice instead of discrete choice, to smooth the discontinuous model in Matsuyama (2007). However, our model is simpler than Matsuyama's in terms of the story and motivation behind the modeling.

To study the complex dynamics in continuous piecewise smooth maps, we adopt two approaches: *border collision bifurcation* and *Markov property*. That is, we obtain two different characterizations of chaotic dynamics in the model. The first approach includes a bifurcation that occurs in piecewise smooth, piecewise linear, and piecewise non-linear maps. This theory reveals the bifurcation from a globally attracting steady state to other non-stationary behaviors using only local information in the system. Especially, we can completely characterize the bifurcation from an attracting steady state to another non-stationary attractor, such as periodic cycles or *chaotic bundles*. Gardini et al. (2008) and Matsuyama et al. (2016) use the border collision bifurcation theory to investigate the chaotic dynamics in their models. Second, we find that our model can have a special property—a Markov property for some sets of parameter values. If the model has such

a property, we can easily establish and characterize its complex dynamics. Yokoo and Ishida (2008) and Asano and Yokoo (2019) find the Markov property in their piecewise linear models to analyze the chaotic dynamics. Therefore, from a technical viewpoint, our model has an advantage against the preceding models because we can characterize the chaotic fluctuations in the model using two different approaches.

The remainder of this paper is organized as follows. Section 2 re-examines the OLG model with a binary choice of technologies. Section 3 derives the piecewise smooth model by introducing a new assumption, a multitude of choices in the technologies, into the OLG model with a binary choice setting. Section 4 describes the border collision bifurcation theory characterized by routes from the globally attracting steady state to other non-stationary cycles, including chaotic fluctuation. Section 5 reveals that the capability of the model has a Markov property for some set of parameter values. Section 6 concludes the study. Some mathematical proofs are delegated to the appendices.

2 The model under binary technology choice

In this section, for the reader's convenience, we re-examine the base model of this study. (See Umezuki and Yokoo (2019) for more details.) We consider a Diamond-type one-sector OLG model that is modified further. Time is discrete, that is, $t = 0, 1, 2, \cdots$, and the agents live for two periods. A young household supplies one unit of labor inelastically. We keep the utility function, u, of the household as simple as possible; this allows us to assume that it is in the form of a log-linearized Cobb-Douglas production function, that is,

$$u(c_t^y, c_{t+1}^o) = (1 - s) \log c_t^y + s \log c_{t+1}^o, \quad s \in (0, 1), \tag{1}$$

where c_t^y denotes the amount of consumption of the young generation born at time t, and c_{t+1}^o denotes the amount of consumption of the old generation living at time $t + 1$. The utility given by Eq.(1) is maximized under the following constraints:

$$c_t^y + s_t = w_t \quad \text{and} \quad c_{t+1}^o = r_{t+1} s_t, \tag{2}$$

where s_t, w_t, and r_{t+1} are the amounts of saving, real wage rate, and real gross rate of return, respectively. The maximization yields

$$s_t = s w_t. \tag{3}$$

The final good, Y_t, which is perishable, is produced by the firm. Unlike the common OLG models, we assume that there are two types of production technologies. We also

assume that, at the beginning of every period, the firm faces a discrete choice problem related to the choice of technology. For simplicity, all the technologies are specified as the Cobb-Douglas of constant returns to scale:

$$Y_t = F_a(K_t, L_t) = AK_t^a L_t^{1-a} \quad \text{and}$$
$$Y_t = F_b(K_t, L_t) = BK_t^b L_t^{1-b},$$

where $A, B > 0$ is the total factor productivity, and $0 < a < b < 1$ is the capital share of the production of technology. In the per-capita form, we can write

$$y_t = f_i(k_t) = F_i(k_t, 1), \tag{4}$$

where $y_t = Y_t/L_t$, $k_t = K_t/L_t$, and $i \in \{a, b\}$. We assume that the firm's owner, who belongs to the old generation, chooses technology that earns the highest return. For simplicity, we assume that when the highest rates of return are tied among two technologies, technology 1 characterized by (a, A) is chosen. Subsequently, the usual first-order conditions with the technology choice are represented by

$$r_t = f'_{J_t}(k_t), \tag{5}$$
$$w_t = f_{J_t}(k_t) - k_t f'_{J_t}(k_t), \quad \text{and} \tag{6}$$
$$J_t = \arg \max_{j \in \{a,b\}} f'_j(k_t). \tag{7}$$

The market clearing condition,

$$k_{t+1} = s_t, \tag{8}$$

with Eqs.(3), (6) and (7) generate the dynamic model in the following form:

$$k_{t+1} = \begin{cases} sA(1-a)k_t^a & 0 \le k_t \le \hat{k}, \\ sB(1-b)k_t^b & \hat{k} < k_t, \end{cases} \tag{9}$$

where

$$\hat{k} = \left[\frac{aA}{bB}\right]^{1/(b-a)}. \tag{10}$$

It is clear that if Eq.(9) has a positive fixed point, it would be globally attracting. As we are interested in non-stationary behaviors, we examine the case where Eq.(9) has no positive fixed point. The following lemma shows that there is a parameter set for which Eq.(9) has no positive fixed point.

Lemma 1. *Let $a, b \in (0, 1)$ with $a < b$, $B > 0$, and $s \in (0, 1)$ be given. Subsequently, there exist $\underline{A} > 0$ and $\overline{A} > 0$ with $\underline{A} < \overline{A}$ such that map (9) has no positive fixed point for $A \in (\underline{A}, \overline{A})$.*

Proof. See Umezuki and Yokoo (2019). □

Finally, by defining a new variable x_t as

$$x_t = \frac{\log\left[k_t/s(1-b)B\hat{k}^b\right]}{\log b(1-a)/a(1-b)},$$ (11)

Eq.(9) can reduce to the following piecewise linear map on the unit interval:

$$x_{t+1} = \tau(x_t) = \begin{cases} 1 + a(x_t - c) & \text{if} \quad 0 \leq x_t \leq c, \\ b(x_t - c) & \text{if} \quad c < x_t \leq 1, \end{cases}$$ (12)

where

$$c = c(s, A) = \frac{\frac{1-b}{b-a}\log\left[aA/bB\right] - \log s(1-b)B}{\log b(1-a)/a(1-b)}.$$ (13)

It is interesting to note that Eq.(12) can be identified with a simplified version of Caianiello's equation in the neural networks, whose original model is proposed by Caianiello to describe the behavior of a "model of brain" or "thinking machine"; this model is studied by Nagumo and Sato (1972) in detail. Additionally, Hata (2014) comprehensively analyzes this type of equation, and we utilize this author's analysis results for the mathematical neuron model to study economic growth.

When investigating Eq.(12), the position of threshold $c(s, A)$ on the unit interval plays an important role. The position of the threshold characterizes the dynamical property of the model. Generally, for a given value of c, Eq.(12) has either a globally attracting periodic cycle or a non-periodic attractor.

The following lemma shows that threshold $c(s, A)$ can take any value within the range of $(0, 1)$, independently of parameters a and b.

Lemma 2. *For any $a, b \in (0, 1)$ with $a < b$ and any $c^* \in (0, 1)$, there exist $s^* \in (0, 1)$ and $A^* \in (\underline{A}, \overline{A})$ such that $c(s^*, A^*) = c^*$.*

Proof. See Umezuki and Yokoo (2019). □

Now, we restate the existence of a periodic orbit in the model.

Proposition 1. *For each irreducible fraction $p/q \in (0, 1)$, there exists a closed interval $\Delta(p/q) \subset (0, 1)$ such that if $c(s, A) \in \Delta(p/q)$, for any $x \in (0, 1)$, the orbit of x converges to some periodic orbit of period q.*

Proof. See Hata (2014), Theorem 4.2 on p.36 and Theorem 10.1 on pp.117–118. □

Thus, we can almost completely grasp the periodic dynamical features of the model by verifying to which closed interval threshold c belongs. Moreover, owing to the piecewise linearity of the model, we can exactly calculate the left and right endpoints of the closed interval $\Delta(p/q)$ for any p/q. See Umezuki and Yokoo (2019) for more details on this point.

Next, we can consider the following set:

$$\Gamma = [0,1] \backslash \bigcup_{p/q \in [0,1] \cap \mathbb{Q}} \Delta(p/q).$$

Set Γ is the remainder obtained from the unit interval $[0,1]$ by Deleting the infinite closed intervals. If $c \in \Gamma$, Eq.(12) has a non-periodic attractor.

Proposition 2. *If $c(s,A) \in \Gamma$, for any $x \in (0,1)$, the ω-limit set of x; that is, $\bigcap_{n=0}^{\infty} \bigcup_{k=n}^{\infty} \mathrm{cl}\tau^k(x)$, is some compact and totally disconnected uncountable set on the unit interval.*

Proof. See Hata (2014), Theorem 7.4 on p.80 and Theorem 8.5 on p.90. □

In the proposition, cl$A$ represents closure of set A. We can conclude that, for $c(s,A) \in \Gamma$, Eq.(12) has a *global* non-periodic attractor; it implies that once such a threshold value is chosen, the economy would fluctuate in a non-periodic manner in the long run for *any* initial condition. However, there is the fact that set Γ is extremely "thin." The Hausdorff dimension of set Γ is zero. This implies that this base model cannot virtually reproduce non-periodic fluctuations in the long run.

3   The model under continuum technology choice

In what follows, we modify the base model examined in the previous section to construct a simple, tractable, OLG model with technology choice to virtually reproduce non-periodic fluctuations in the long run.

To do this, we make only one modification. We assume that the firm faces a continuum of technologies. That is, there is a continuum of production functions,

$$Y_t = F_\alpha(K_t, L_t) = A K_t^\alpha L_t^{1-\alpha}, \qquad \alpha \in [a,b],$$

and the firm can choose this before the production of a good. Here, we also assume that the parameter of total factor productivity, given as A and B in the binary choice setting, is constant through all technologies.

Therefore, we face the dynamic model in the following form:

$$\begin{cases} k_{t+1} = sA(1-\alpha)k_t^\alpha, \\ \alpha = \arg\max_{\alpha^* \in [a,b]} \left\{ A\alpha^* k_t^{\alpha^*-1} \right\}, \quad \text{and} \quad k_0 > 0. \end{cases} \tag{14}$$

It is easily shown that α is given by

$$\alpha = \begin{cases} a, & k_t \leq e^{-\frac{1}{a}}, \\ -\frac{1}{\log k_t}, & \text{if} \quad e^{-\frac{1}{a}} < k_t \leq e^{-\frac{1}{b}}, \\ b, & e^{-\frac{1}{b}} < k_t. \end{cases} \tag{15}$$

Subsequently, we have the following piecewise-smooth dynamic model:

$$k_{t+1} = \begin{cases} \beta(1-a)k_t^a, & k_t \leq e^{-\frac{1}{a}}, \\ \beta\left(1 + \frac{1}{\log k_t}\right)k_t^{-\frac{1}{\log k_t}}, & \text{if} \quad e^{-\frac{1}{a}} < k_t \leq e^{-\frac{1}{b}}, \\ \beta(1-b)k_t^b, & e^{-\frac{1}{b}} < k_t, \end{cases} \tag{16}$$

where $\beta = sA$.

By defining a new variable $y_t = \log k_t$, Eq.(16) turns out to be

$$y_{t+1} = h(y_t) = \begin{cases} h_1(y_t) = ay_t + \log\beta(1-a), & y_t \leq -\frac{1}{a}, \\ h_2(y_t) = \log(1 + \frac{1}{y_t}) + \log\beta - 1, & \text{if} \quad -\frac{1}{a} < y_t \leq -\frac{1}{b}, \\ h_3(y_t) = by_t + \log\beta(1-b), & -\frac{1}{b} < y_t. \end{cases} \tag{17}$$

Fig.1 depicts the graph of return map of y_t, which has a fixed point in $\left(-\frac{1}{a}, -\frac{1}{b}\right)$.

<<insert Fig.1 around here>>

The graphical argument shows that if Eq.(17) has a fixed point on $\left(-\infty, -\frac{1}{a}\right]$ or $\left[-\frac{1}{b}, \infty\right)$, it would be globally attracting. Elementary algebra shows the following proposition that detects the set of parameter $\beta = sA$, for which the model exhibits the globally attracting steady state.

Proposition 3. *Let*

$$\beta^*(u, v) = \frac{1}{1-v}\exp\left(-\frac{1-u}{u}\right), \quad 0 < u, v < 1.$$

For any $a < b$, if $\beta < \beta^*(a, a)$ or $\beta^*(b, b) < \beta$, map (17) has a fixed point on $\left(-\infty, -\frac{1}{a}\right]$ or $\left[-\frac{1}{b}, \infty\right)$, respectively.

Here, it should be noted that, for any $a < b$, we have $\beta^*(a, a) < \beta^*(b, b)$.

As we are interested in non-stationary behaviors, we examine the case wherein Eq.(17) has a positive steady state on the interval $\left(-\frac{1}{a}, -\frac{1}{b}\right)$. That is, we mainly focus on the following case:

$$\beta^*(a, a) < \beta < \beta^*(b, b).$$

Let us further classify the model. It is evident that every trajectory generated by (17) eventually enters the trapping interval $T = \left[h_2(-\frac{1}{b}), h_1(-\frac{1}{a})\right]$ and never leaves it. Thus, to study the long-run behavior of the model in this situation, it is sufficient to focus on the dynamics of the trapping interval, I. It must be noted that, depending on parameter values a and b, we face the following two scenarios.

1. If $\dfrac{a-b}{ab} > \log\dfrac{(1-b)}{(1-a)}$, then $\beta^*(b,a) < \beta^*(a.b)$. We have the following cases:

- If $\beta^*(a,a) < \beta < \beta^*(b,a)$, then T contains the right threshold only.
- If $\beta^*(b,a) < \beta < \beta^*(a,b)$, then T contains all the thresholds.
- If $\beta^*(a,b) < \beta < \beta^*(b,b)$, then T contains the left threshold only.

2. If $\dfrac{a-b}{ab} < \log\dfrac{(1-b)}{(1-a)}$, then $\beta^*(a,b) < \beta^*(b.a)$. We have the following cases:

- If $\beta^*(a,a) < \beta < \beta^*(a,b)$, then T contains the right threshold only.
- If $\beta^*(a,b) < \beta < \beta^*(b,a)$, then T contains no thresholds.
- If $\beta^*(b,a) < \beta < \beta^*(b,b)$, then T contains the left threshold only.

If T contains only the right (left) threshold, the model can be regarded as a unimodal map. On the other hand, if T contains both thresholds, the model reduces to a bimodal map on the unit interval. Finally, if T contains no thresholds, the model can be regarded as a monotonically decreasing map, which can have a periodic cycle at most period two. It is reasonable that we omit such an insignificant case.

As we will see later, both unimodal and bimodal maps in our model are capable of generating chaotic behaviors. We investigate the chaotic dynamics of the unimodal and bimodal cases in sections 4 and section 5, respectively.

4 Chaotic dynamics: Border collision bifurcation

In this study, we adopt two approaches to investigate the chaotic behaviors in the model. In this section, we deal with *border collision bifurcation* to investigate the dynamical property of the unimodal case. In this case, we can locally, but almost completely, characterize the bifurcation from a globally attracting steady state to non-stationary behaviors; that is, bifurcation from a globally attracting steady state to a periodic cycle or a *chaotic bundle*. Roughly speaking, a one-dimensional piecewise map may undergo border collision bifurcation when the 45 degree line touches the graph of the map at its non-smooth boundaries. Therefore, in our model, border collision bifurcation occurs when β exceeds

$\beta^*(a, a)$ as well as β approaches $\beta^*(b, b)$. To avoid increasing the length of the paper, we focus on the former case, in which the model can be represented by a single peaked uni-modal map. Of course, the same analytical method is adopted for the latter case, in which the model can be represented by a *V*-shaped unimodal map. In section 4.1, we briefly discuss some mathematical results for border collision bifurcation. In section 4.2, we adopt the results to our OLG model with technology choice.

4.1   Some mathematical results from border collision bifurcation

All results in this section follow from Nusse and Yorke (1995).

Before we examine the piecewise smooth map (17), we consider the following piecewise linear map:

$$F_{v_1,v_2} = \begin{cases} v_1 x + 1 & x \leq 0, \\ v_2 x + 1 & 0 < x, \end{cases} \tag{18}$$

with $0 < v_1 < 1$ and $v_2 < -1$. For convenience, let

$$D = \{(v_1, v_2) : 0 < v_1 < 1 \quad \text{and} \quad v_2 < -1\}.$$

Note that the above map is typologically conjugated with the following map:

$$F_\mu = \begin{cases} v_1 x + \mu & x \leq 0 \\ v_2 x + \mu & 0 < x, \end{cases} \tag{19}$$

for all $\mu > 0$, which undergoes border collision bifurcation when $\mu = 0$.

First, we state the existence of the periodic orbit in map (18).

Theorem 1. (Nusse and Yorke, 1995)
For integer $m \geq 2$, let

$$P_m = \left\{ (v_1, v_2) \in D : -v_1^{1-m} < v_2 < \frac{1 - v_1^{m-1}}{v_1^{m-1} - v_1^{m-2}} \right\}.$$

If $(v_1, v_2) \in P_m$, F_{v_1,v_2} has a period-m attractor. Moreover, the set

$$\{x : \omega\text{-limit set of } x \text{ is not the period-m attractor}\}$$

Has Lebesgue measure zero.

Proof. See Nusse and Yorke (1995).   □

Let γ_m be the intersection of $v_2 = -v_1^{1-m}$ and $v_2 = \frac{1-v_1^{m-1}}{v_1^{m-1}-v_1^{m-2}}$. Note that, for any integer $m \geq 2$, $\gamma_{m+1} < \gamma_m$. Moreover, if $v_1 \leq \gamma_N$ for some N,

$$-v_1^{1-(m+1)} < \frac{1-v_1^{(m+1)-1}}{v_1^{(m+1)-1} - v_1^{(m+1)-2}} < -v_1^{1-m} < \frac{1-v_1^{m-1}}{v_1^{m-1} - v_1^{m-2}}$$

for any $m < N$. Therefore, the family of sets P_m is pairwise disjoint. Fig.2 depicts the P_2, P_3, P_4, and P_5 on the (v_1, v_2)-plane.

<<insert Fig.2 around here>>

Next, it is reasonable that we examine the case wherein $(v_1, v_2) \in D \setminus \bigcup_{m \geq 2} P_m := \Sigma$. That is, if $(v_1, v_2) \in \Sigma$, map F_{v_1, v_2} has a chaotic attractor in the sense that there exist no periodic attractors, and, for any x, the trajectory of x has a positive Lyapunov exponent. Hereafter, we call set Σ the *chaotic region*. Moreover, if $\left(v_1^0, v_2^0\right) \in \Sigma$, we call such a pair the *chaotic pair*.

We discuss the chaotic region for more details. Let $\left(v_1^0, v_2^0\right)$ be any given chaotic pair. Define $L\left(v_1^0\right)$ for the intersection of the vertical line and chaotic region, that is,

$$L\left(v_1^0\right) = \left\{ (v_1, v_2) \in \Sigma : v_1 = v_1^0 \right\}.$$

Let m be the integer for which the "top" of the component of $L\left(v_1^0\right)$ that contains $\left(v_1^0, v_2^0\right)$ is the boundary of set P_m. Moreover, let $C_m\left(v_1^0\right)$ be this component of $L\left(v_1^0\right)$. It is clear that there are two cases wherein $C_m\left(v_1^0\right)$ is bounded or unbounded. Fig.3 depicts some examples of set C_m on the (v_1, v_2)-plane.

<<insert Fig.3 around here>>

As we will see later, in our model, we only have to consider the case wherein $m = 2$ and $C_m\left(v_1^0\right)$ is unbound. Therefore, we simply define $C_m\left(v_1^0\right)$ as $C\left(v_1^0\right)$. Considering this, we state the existence of the chaotic orbit in map (18) as follows.

Theorem 2. (Nusse and Yorke, 1995, with some modifications[1])
Let $(v_1, v_2) \in C$ be a chaotic pair and assume that $(v_1, v_2) \in C(v_1)$. There exist $(v_1, \bar{v}_2) \in C(v_1)$ and $(v_1, \hat{v}_2) \in C(v_1)$, for which $\bar{v} < \hat{v} < -v_1^{-1}$ such that the following hold.

1. *If $\hat{v} < v_2 < -v_1^{-1}$, map F_{v_1, v_2} has a 2^{k+1}-piece chaotic attractor for some $k \geq 1$ (depending on v_1 and v_2). In addition, if $v_1^2 < \frac{1}{2}\left(\sqrt{5} - 1\right)$, then $k = 1$.*

---

[1]Here, we only consider the case wherein $m = 2$ and $C_m\left(v_1^0\right)$ is unbounded.

2. *If $\bar{v} < v_2 < \hat{v}$, then F_{v_1,v_2} has a two-piece chaotic attractor.*

3. *If $v_2 < \bar{v}$, then F_{v_1,v_2} has an one-piece chaotic attractor.*

Proof. See Nusse and Yorke (1995). □

We have seen the periodic and chaotic dynamics generated from border collision bifurcation on the piecewise linear map (18). The following theorem translates the above results to general border collision bifurcation results for piecewise, smooth, one-dimensional nonlinear maps.

Theorem 3. (Nusse and Yorke, 1995)
Let $G : \mathbb{R} \times J \to \mathbb{R}$ be a piecewise smooth map. Assume that G has the isolated crossing fixed-point property at (x_0, μ_0). Let $m \geq 2$ and $k \geq 2$ be any integers. Define $v_1 = \lim_{x \uparrow x_0} \frac{\partial G}{\partial x}(x, \mu_0)$ and $v_2 = \lim_{x \downarrow x_0} \frac{\partial G}{\partial x}(x, \mu_0)$. Then,

(i) *if $(v_1, v_2) \in P_m$, G exhibits border-collision bifurcation from a fixed-point attractor to a period-m attractor at $(x, \mu) = (x_0, \mu_0)$.*

(ii) *if $(v_1, v_2) \in \Sigma_k$, where $\Sigma_k = \text{Int}\{(v_1, v_2) \in \Sigma : F_{v_1,v_2} \text{ has a k-piece chaotic attractor}\}$, G exhibits a border-collision bifurcation from a fixed point attractor to a k-piece chaotic attractor at $(x, \mu) = (x_0, \mu_0)$.*

Proof. See Nusse and Yorke (1995). □

The property called the *isolated crossing fixed-point property* may be a somewhat unfamiliar notion; however, it is not an unusual property. Indeed, our model has this property and can be adopted to Theorem 3.

Proposition 4. *Map (17) has the isolated crossing fixed-point property at $(y, \beta) = \left(-\frac{1}{a}, \beta^*(a, a)\right)$.*

Proof. See Appendix. □

4.2 Border collision bifurcation on the OLG model.

In this section, we detect the periodic and chaotic dynamics generated from the border collision bifurcation in our model.

We now consider the following unimodal map:

$$y_{t+1} = h(y_t) = \begin{cases} h_1(y_t) = ay_t + \log\beta(1-a) & y_t \leq -\frac{1}{a}, \\ h_2(y_t) = \log(1 + \frac{1}{y_t}) + \log\beta - 1 & -\frac{1}{a} < y_t \leq -\frac{1}{b}. \end{cases} \quad (20)$$

As we have seen in Proposition 4, map (20) has the isolated crossing fixed-point property at $(y, \beta) = \left(-\frac{1}{a}, \beta^*(a, a)\right)$, and therefore we can adopt Theorem 3 into the model. Now, we have the following:

$$v_1 = \lim_{y \uparrow -\frac{1}{a}} \frac{\partial h}{\partial y}(x, \beta^*(a, a)) = a \quad \text{and} \tag{21}$$

$$v_2 = \lim_{y \downarrow -\frac{1}{a}} \frac{\partial h}{\partial y}(x, \beta^*(a, a)) = -\frac{a^2}{1-a}. \tag{22}$$

It should be noted that, in our model, we cannot take v_1 and v_2 independently. Fig.4 depicts line

$$v_2 = -\frac{v_1^2}{1 - v_1}, \tag{23}$$

on the (v_1, v_2)-plane. We have only to examine the parameter set of (v_1, v_2) on this line. In the figure, the left white circle represents intersections of two lines, $v_2 = -1$ and (23). On the other hand, the right white circle represents intersections of two lines, $v_2 = -\frac{1}{v_1}$ and (23). The v_1 coordinate of the left and the right white circles are given by v^* and v^{**}, respectively. Subsequently, we easily see that $v^* = \frac{-1+\sqrt{5}}{2} \approx 0.618$, and $v^{**} \approx 0.682$ which is a root of the equation $v_1^3 + v_1 - 1 = 0$ in $[0, 1]$.

<<insert Fig.4 around here>>

First, we can immediately state the periodic cycle in our model.

Proposition 5. *If $a \in (v^*, v^{**})$, our model exhibits border collision bifurcation from an attracting fixed point to a period-two attractor at $(y, \beta) = (-1/a, \beta^*(a, a))$.*

We now examine the chaotic dynamics in the model, which is the main focus of this section. It is easy to see that that our model exhibits the chaotic attractor for $a > v^{**}$. Moreover, we see that we have to only consider sets $C_2(a)$ for $a > v^{**}$, which are unbounded. According to Theorems 2 and 3, we expect that the model exhibits a 2^{k+1}-piece chaotic attractor for some $k \geq 1$ (depending on v_1 and v_2), a two-piece chaotic attractor, or a one-piece chaotic attractor.

Fortunately, Sushko et al. (2015) comprehensively analyze the border collision bifurcation in piecewise linear map (18). Their results are too technical to refer to all of them here; however, we need to refer to a few results to investigate the chaotic dynamics in our model. Now, we define the following sets:

$$Q_1 = \left\{ (v_1, v_2) \in \Sigma : v_1 v_2^2 - v_1 + v_2 < 0 \right\},$$

$$Q_2 = \left\{ (v_1, v_2) \in \Sigma : v_1 v_2^2 - v_1 + v_2 > 0, v_1^2 v_2^3 + v_1 - v_2 < 0 \right\}, \quad \text{and}$$

$$Q_4 = \left\{ (v_1, v_2) \in \Sigma : v_1^2 v_2^3 + v_1 - v_2 > 0, v_1^6 v_2^6 - v_1 + v_2 < 0 \right\}.$$

Subsequently, we have the following.

Theorem 4. *For $k = 1, 2,$ and 4, if $(v_1, v_2) \in Q_k$, map (18) has the k-piece chaotic attractor.*

Proof. See Sushko et al. (2015). □

Fig.5 depicts the sets $Q_1, Q_2,$ and Q_4 on the (v_1, v_2)-plane. Black circles represent the intersections of line $v_2 = -\frac{v_1^2}{1 - v_1}$ and the boundaries of Q_k ($k = 1, 2, 4$). The v_1 coordinate of these intersections, represented by σ^* and σ^{**}, are as follows:

- $\sigma^* \approx 0.705$ is a root of the equation $v_1^8 - v_1^3 + 2v_1^2 - v_1 = 0$ in $[0, 1]$.

- $\sigma^{**} \approx 0.724$ is a root of the equation $v_1^5 + v_1^2 - v_1 = 0$ in $[0, 1]$.

<<insert Fig.5 around here>>

Now, we can completely characterize the chaotic dynamics generated from border collision bifurcation in our OLG model.

Proposition 6. *For map (20), we have the following three scenarios of bifurcation from the attracting fixed point to a chaotic attractor.*

1. *For $a \in (v^{**}, \sigma^*)$, our model exhibits border collision bifurcation from the attracting fixed point to a four-piece chaotic attractor at $(y, \beta) = (-1/a, \beta^*(a, a))$.*

2. *For $a \in (\sigma^*, \sigma^{**})$, our model exhibits border collision bifurcation from the attracting fixed point to a two-piece chaotic attractor at $(y, \beta) = (-1/a, \beta^*(a, a))$.*

3. *For $a \in (\sigma^{**}, 1)$, our model exhibits border collision bifurcation from the attracting fixed point to an one-piece chaotic attractor at $(y, \beta) = (-1/a, \beta^*(a, a))$.*

On a k-piece chaotic attractor, the trajectory goes through each interval every k-th period. Of course, when a trajectory returns to the same interval, it never takes the same value. Interestingly, when observing such a trajectory, one may regard the trajectory as a k-cycle with random noises. Fig.6 (a) depicts the bifurcation diagram of map (20) respect to β, where the model has the capability to exhibit four-piece chaotic attractor. Fig.6 (b) depicts time series obtained from map (20) with four-piece chaotic attractor.

<<insert Fig.6 around here>>

In this section, we observed the chaotic dynamics where $\beta \in (\beta^*(a, a), \beta^*(a, a) + \epsilon)$ and, eventually, $\beta \in (\beta^*(b, b) - \epsilon, \beta^*(b, b))$. In other words, we have investigated the *beginning* and *end* of the chaotic dynamics in the OLG model with technology choice. In the next section, we examine the case wherein the β is not sufficiently near $\beta^*(a, a)$ or $\beta^*(b, b)$.

5 Chaotic dynamics : Markov property

In this section, we show that our model has the *Markov property* for some sets of parameters, wherein the model can reduce to a bimodal map on the unit interval. If the map has such a property, we can easily reproduce chaotic dynamics. In what follows, we assume

$$\frac{a - b}{ab} > \log \frac{1 - b}{1 - a} \quad \text{and} \quad \beta^*(b, a) < \beta < \beta^*(a, b),$$

where the model can be reduce to a bimodal map on the unit interval.

To simplify the analysis of the dynamics, we first use a variable change to reduce our model to the bimodal map in the unit interval.

By defining a new variable x_t as

$$x_t = \frac{y_t + 1 - \log \beta(1 - b)}{\log(1 - a) - \log(1 - b)},$$

Eq.(16) can be transformed into the following piecewise smooth map:

$$x_{t+1} = f(x_t) = \begin{cases} f_L(x_t) = 1 + a(x_t - \theta_L), & x_t \leq \theta_L, \\ \phi(x_t), & \theta_L < x_t \leq \theta_R, \\ f_R(x_t) = b(x_t - \theta_R), & \theta_R < x_t, \end{cases} \tag{24}$$

where

$$\phi(x_t) = \log \left[\frac{g(x_t)}{(1 - b)(g(x_t) - 1)} \right]^{\frac{1}{\lambda}}, \quad \text{with}$$

$$\lambda = \log \frac{(1 - a)}{(1 - b)},$$

$$g(x_t) = \lambda x_t + \log \beta(1 - b),$$

and

$$\theta_L = -\frac{(1 - a) + a \log \beta(1 - b)}{\lambda a},$$

$$\theta_R = -\frac{(1 - b) + b \log \beta(1 - b)}{\lambda b}.$$

Now, we briefly discuss some property of map (24). It is easily shown that

$$\frac{d\phi(x)}{dx}(\theta_L) = -\frac{a^2}{1-a} \quad \text{and}$$
$$\frac{d\phi(x)}{dx}(\theta_R) = -\frac{b^2}{1-b}.$$

Moreover, we have the following.

Proposition 7. *Map $\phi(x)$ is a monotonically decreasing and concave function on (θ_L, θ_R).*

Proof. See Appendix. □

Therefore, the derivatives of ϕ have lower bound $-\frac{b^2}{1-b}$ and upper bound $-\frac{a^2}{1-a}$ for $x \in [\theta_L, \theta_R]$.

5.1 Mathematical definition of the Markov property

First, we give some mathematical definitions of the Markov property. See, for example, Boyarsky and Góra (1997) for more details. Let $I = [0, 1]$ and $\psi : I \to I$ be a map on I onto itself. Let $\mathcal{P}$ be a finite partition of I and I_k ($k = 1, 2, \ldots, n$) be subintervals of the partition. Moreover, let ψ_k be the restriction of ψ to I_k. Now, we can define the following.

Definition 1. *If each ψ_k is a homeomorphism from I_k onto some connected union of subintervals I_m, then ψ is said to be Markov. Partition $\mathcal{P}$ is said to be a Markov partition with respect to ψ.*

To examine complex dynamics in the piecewise smooth map, we also need to discuss the following property. Here, let ψ be a piecewise smooth map, which is not necessarily Markov, and let ψ^n be an n-th iterate of map ψ. Then, we define the following.

Definition 2. *If there is an integer $n \geq 1$ such that $\inf \left| \frac{d\psi^n(x)}{dx} \right| > 1$ on each I_k whenever the derivative exists, then ψ is said to be eventually expanding.*

It is readily seen that the eventual expansion implies that the map has no attracting periodic cycles and exhibits chaotic dynamics with long-run observability.

5.2 Markov partition on the OLG model

We first show that our model (24) can exhibit the following periodic cycle for some set of parameter values:

$$0 = f^5(0) < f^2(0) = \theta_L < f^4(0) = \theta_R < f(0) = c < f^3(0) = 1. \tag{25}$$

Fig.7 depicts the graph of return map of x_t with the periodic cycle (25). We can show that such a specific cycle implies chaotic dynamics.

<<insert Fig.7 around here>>

Proposition 8. *(Observable chaos on a period-5 Markov partition)*
There exist a_L and a_R with $< 0 a_L < a_R < 1$. If $a \in (a_L, a_R)$, there exists $b \in (a, 1)$ and
$\beta > 0$ such that for (a, b, β), we have a period-5 Markov partition of the unit interval with
respect to f. Moreover, f is eventually expanding and thus exhibits observable chaos.

Proof. To calculate the period-5 cycle given by (25), θ_L and θ_R must solve the following
equations,

$$f_R(1) = \theta_R \quad \text{and} \quad f_R(f_L(0)) = \theta_L.$$

A straightforward calculation shows that

$$\beta = \frac{1}{1 - b} \exp - \left[\frac{b\lambda}{1 + b} + \frac{1 - b}{b} \right] \quad \text{and} \tag{26}$$

$$\lambda = \frac{(b - a)(ab + 1)(1 + b)}{a^2 b^3}. \tag{27}$$

First, we check that

$$\beta^*(b, a) < \frac{1}{1 - b} \exp - \left[\frac{b\lambda}{1 + b} + \frac{1 - b}{b} \right] < \beta^*(a, b). \tag{28}$$

We see that the inequality

$$\beta^*(b, a) < \frac{1}{1 - b} \exp - \left[\frac{b\lambda}{1 + b} + \frac{1 - b}{b} \right]$$

holds if and only if $0 < \frac{\lambda}{1+b}$. Thus, clearly, this inequality holds. Moreover, we see that
the inequality

$$\frac{1}{1 - b} \exp - \left[\frac{b\lambda}{1 + b} + \frac{1 - b}{b} \right] < \beta^*(a, b)$$

holds if and only if $\log \frac{1-b}{1-a} < \frac{a-b}{ab} \frac{1+b}{b}$. Let

$$\eta_1(b) = \log \frac{1 - b}{1 - a} \quad \text{and} \quad \eta_2(b) = \frac{a - b}{ab} \frac{1 + b}{b}.$$

It is easily seen that $\eta_1(b)$ is a monotonically decreasing and concave function in $[0, 1]$.
Moreover, we have

$$\frac{d\eta_2(a)}{db} = -\frac{1 + a}{a^3} < 0 \quad \text{and} \tag{29}$$

$$\frac{d^2\eta_2(a)}{db^2} = \frac{2(a + 2)}{a^4} > 0. \tag{30}$$

Therefore, there exists $\epsilon > 0$ such that for any $a \in (0, 1)$, $\eta_2(b)$ is a monotonically decreasing and convex function for $b \in (a - \epsilon, a + \epsilon)$. Note that $\eta_1(a) = \eta_2(a)$ and

$$\frac{d\eta_1(a)}{db} = -\frac{1}{1 - a} \quad \text{and} \quad \frac{d\eta_2(a)}{db} = -\frac{1 + a}{a^3}.$$

Considering the concavity of η_1 and convexity of η_2 for neighborhood a, if

$$-\frac{1}{1 - a} < -\frac{1 + a}{a^3} \Rightarrow a^3 + a^2 - 1 > 0,$$

there exists $a < \bar{a}$ such that $\log \frac{1-b}{1-a} < \frac{a-b}{ab} \frac{1+b}{b}$ for $b \in (a, \bar{a})$. Let $a_L \approx 0.755$ be a root of the equation $a^3 + a^2 - 1 = 0$ in $(0, 1)$. We conclude that if $a \in (a_L, \bar{a})$, then inequality (28) holds.

Next, we examine Eq.(27). Let

$$\varphi_1(b) = \log \frac{1 - a}{1 - b} \quad \text{and} \quad \varphi_2(b) = \frac{(b - a)(ab + 1)(1 + b)}{a^2 b^3}.$$

Clearly, $\varphi_1(a) = \varphi_2(a)$, and we can easily see that $\varphi_1(b)$ is a monotonically increasing convex function and $\lim_{b=1} \varphi_1(b) = \infty$. Moreover, we have

$$\varphi_2(1) = \frac{2(1 - a^2)}{a^2} \quad \text{is bounded for } a \in (0, 1) \text{ and}$$

$$\frac{d\varphi_2(a)}{db} = \frac{a^3 + a^2 + a + 1}{a^5} > 0.$$

Therefore, if

$$\frac{d\varphi_1(a)}{db} = \frac{1}{1 - a} < \frac{a^3 + a^2 + a + 1}{a^5} \Rightarrow a^5 + a^4 - 1 < 0,$$

$\varphi_1(b)$ intersects with $\varphi_2(b)$ at least one point $b \in (a, 1)$. Let $\hat{a} \approx 0.857$ be a root of the equation $a^5 + a^4 - 1 = 0$ in $(0, 1)$. We conclude that if $a < \hat{a}$, there exists $b \in (a, 1)$ such that, for a and b, Eq.(27) holds.

Let $a_R = \min\{\bar{a}, \hat{a}\}$. Now, we can state that if $a \in (a_L, a_R)$, there exists $b \in (a, 1)$ and $\beta > 0$ such that for (a, b, β), we have a period-5 Markov partition of the unit interval with respect to f.

Finally, we show that f is eventually expanding. Let $I_1 = [0, \theta_L], I_2 = [\theta_L, \theta_R], I_3 = [\theta_R, c], I_4 = [c, 0]$, and $\bar{I}_k$ be an interior of I_k. Note that every point $x \in \bigcup_{k=1}^{k} \bar{I}_k$ will visit I_2 at least once every fourth iteration. Therefore, for $x \in \bigcup_{k=1}^{k} \bar{I}_k$,

$$\left| (f^4)'(x) \right| \geq a^3 |\phi'| \geq \left| -\frac{a^5}{1 - a} \right|,$$

and if

$$\left| -\frac{a^5}{1-a} \right| > 1 \Rightarrow a^5 + a - 1 > 0, \tag{31}$$

map f is eventually expanding. Since we can easily check whether $a_L < a$, inequality (31) holds, which completes the proof. $\qquad\square$

Proposition 8 can be immediately extended to a more general case of a period-$(2n + 3)$ Markov partition for $n \geq 1$.

Proposition 9. *(Observable chaos on a period-$(2n + 3)$ Markov partition)*
For any $n \in \mathbb{N}$, there exist $a_{2n+3,L}$ and $a_{2n+3,R}$ with $0 < a_{2n+3,L} < a_{2n+3,R} < 1$. If $a \in (a_{2n+3,L}, a_{2n+3,R})$, there exists $b \in (a, 1)$ and $\beta > 0$ such that for (a, b, β), we have a period-$(2n + 3)$ Markov partition of the unit interval with respect to f. Moreover, f is eventually expanding and, hence, chaotic.

Proof. See Appendix. $\qquad\square$

6 Concluding remarks

Based on the model studied by Umezuki and Yokoo (2019), we develop a piecewise smooth OLG model. By assuming a continuous choice instead of discrete choice of the technologies, the model has the capability to exhibit several dynamic growth patterns, including chaotic dynamics, which cannot be observed virtually for the model in Umezuki and Yokoo (2019). Moreover, in spite of its generality, the model is tractable enough to analytically investigate such complex dynamics in depth.

First, by using the border collision bifurcation theory, we investigated the routes from a globally attracting steady state to other non-stationary behaviors. Then, we completely characterized the chaotic dynamics around the bifurcation point; that is, we detected four-piece, two-piece, and one-piece chaotic attractors. Second, we calculated the parameter values for which the model has the Markov property. Then, we characterized the chaotic dynamics, which are different from those in the case of border collision bifurcation. However, one might argue that sets of the parameter value, for which the map is Markov, are too restricted. For future research, it is a natural task to check the *robustness* of the chaotic dynamics by characterizing the dynamics near the parameter values for which the map is Markov.

Finally, it should be pointed out that, compared with the output elasticity for capital (or labor) estimated in the real world, parameter values a and b, for which the model can exhibit chaotic dynamics, are relatively high. Although the intuition behind this remains

unclear, from the technical view point, it could be explained by considering an inverse problem as follows. In this study, we assume that the total factor productivity of the technology, represented by A, is constant for all technologies. However, in general, we can consider different total factor productivity for each technology. In that case, the model has more flexibility, and various new problems might appear, including the following. "A set of which type of technologies is needed to reduce the model to a continuous piecewise linear map?" "For a given piecewise smooth map, is there a set of technologies such that the model can be reduced to the given piecewise smooth map?" "If so, what features does the set of technologies have?" In the future, we hope that our model is investigated more deeply with additional settings without losing its tractability and generality.

Appendix A   Proof of Proposition 4

Proof. For a general statement of the isolated crossing fixed-point property, see Nusse and Yorke (1995). Map (20) has the isolated crossing fixed-point property at $\left(-\frac{1}{a}, \beta^*(a, a)\right)$ if the following conditions hold.

1. There exists $\left\{\left(-\frac{1}{a}, \beta\right) : \beta \in J_0, \; J_0 \text{ is an open interval containing } \beta^*(a, a)\right\}$, and for any $\beta \in J_0$, map (20) is not differentiable at the point $\left(-\frac{1}{a}, \beta\right)$.

2. The set $\{(x(\beta), \beta) : h(x(\beta)) = x(\beta), \beta \in J_0\}$ is a continuous curve and intersects curve $\left\{\left(-\frac{1}{a}, \beta\right) : \beta \in J_0\right\}$ transversally at $\left(-\frac{1}{a}, \beta\right)$.

3. For $\beta \in J_0$, $\frac{dh(y)}{dy} > 0$ for $y < -\frac{1}{a}$ and $\frac{dh(y)}{dy} < 0$ for $y > -\frac{1}{a}$. Moreover, the left limit $\lim_{y \uparrow -\frac{1}{a}} \frac{dh(y)}{dy}$ and right limit $\lim_{y \downarrow -\frac{1}{a}} \frac{dh(y)}{dy}$ exist.

4. $h\left(-\frac{1}{a}\right)$ is a smooth function of $\beta \in J_0$, and for $\beta = \beta^*(a, a)$, $\frac{dh\left(-\frac{1}{a}\right)}{d\beta} > 0$.

It is obvious that map (20) satisfies these conditions. □

Appendix B   Proof of Proposition 7

Proof. We easily show that

$$\frac{d\phi(x)}{dx} = -\frac{1}{g(x)[g(x) - 1]}.$$

Since $\lambda > 0$ and $g(\theta_R) = -\frac{b}{1-b} < 0$, $g(x) < 0$ for $[\theta_L, \theta_R]$. Therefore, we have

$$\frac{d\phi(x)}{dx} < 0.$$

Moreover, we have

$$\frac{d^2\phi(x)}{dx^2} = \frac{\lambda[2g(x)-1]}{g(x)^2[g(x)-1]^2} < 0,$$

for $x \in [\theta_L, \theta_R]$. This completes the proof. $\square$

Appendix C Proof of Proposition 9

Proof. First, we show that there exists the following $2n+3$ cycle:

$$0 = f^{2n+3}(0) < f^{n+1}(0) = \theta_L < f^{2n+2}(0) = \theta_R < \cdots < f^{n+3}(0) < f(0) < 1 = f^{n+2}(0). \tag{C.1}$$

To calculate the cycle given by (C.1), θ_L and θ_R must solve the following equations:

$$f_R^n(1) = \theta_R \quad \text{and} \quad f_R^n(f_L(0)) = \theta_L.$$

A straightforward but tedious calculation shows that

$$\beta = \frac{1}{1-b}\exp-\left[\frac{b^n\lambda}{\Sigma_{k=0}^n b^k} + \frac{1-b}{b}\right] \quad \text{and} \tag{C.2}$$

$$\lambda = \frac{(b-a)(1+ab^n)\Sigma_{k=0}^n b^k}{a^2 b^{2n+1}}. \tag{C.3}$$

First, we check that

$$\beta^*(b,a) < \frac{1}{1-b}\exp-\left[\frac{b^n\lambda}{\Sigma_{k=0}^n b^k} + \frac{1-b}{b}\right] < \beta^*(a,b). \tag{C.4}$$

We see that the inequality

$$\beta^*(b,a) < \frac{1}{1-b}\exp-\left[\frac{b^n\lambda}{\Sigma_{k=0}^n b^k} + \frac{1-b}{b}\right]$$

holds if and only if

$$0 < \lambda\left(\frac{b^n}{\Sigma_{k=0}^n b^k}\right).$$

Clearly, this inequality holds. Moreover, we also see that the inequality

$$\frac{1}{1-b}\exp-\left[\frac{b^n\lambda}{\Sigma_{k=0}^n b^k} + \frac{1-b}{b}\right] < \beta^*(a,b)$$

holds if and only if $\log\frac{1-b}{1-a} < \frac{a-b}{ab}\frac{\Sigma_{k=0}^n b^k}{b^n}$. Let

$$\eta_1(b) = \log\frac{1-b}{1-a} \quad \text{and} \quad \hat{\eta}_2(b) = \frac{a-b}{ab}\frac{\Sigma_{k=0}^n b^k}{b^n}.$$

It is easily seen that $\eta_1(b)$ is a monotonically decreasing and concave function in $[0, 1]$. Moreover, we have

$$\frac{d\hat{\eta}_2(a)}{db} = -\frac{\Sigma_{k=0}^n a^k}{a^{n+2}} < 0 \quad \text{and} \tag{C.5}$$

$$\frac{d^2\hat{\eta}_2(a)}{db^2} = \frac{(1+n)(1+a^{n+1}) + 2\Sigma_{k=1}^n (n-k+1)a^k}{a^{n+3}} > 0. \tag{C.6}$$

Therefore, there exists $\epsilon > 0$ such that for any $a \in (0, 1)$, $\eta_2(b)$ is a monotonically decreasing and convex function for $b \in (a - \epsilon, a + \epsilon)$. Note that $\eta_1(a) = \hat{\eta}_2(a)$, and

$$\frac{d\eta_1(a)}{db} = -\frac{1}{1-a} \quad \text{and} \quad \frac{d\hat{\eta}_2(a)}{db} = -\frac{\Sigma_{k=0}^n a^k}{a^{n+2}}.$$

Considering the concavity of η_1 and convexity of $\hat{\eta}_2$ for neighborhood a, if

$$-\frac{1}{1-a} < -\frac{\Sigma_{k=0}^n a^k}{a^{n+2}} \Rightarrow a^{n+2} + a^{n+1} - 1 > 0,$$

there exists $a < \bar{a}_{2n+3}$ such that $\log \frac{1-b}{1-a} < \frac{a-b}{ab} \frac{\Sigma_{k=0}^n b^k}{b^n}$ for $b \in (a, \bar{a}_{2n+3})$. Let $a_{2n+3,L}$ be a root of the equation $a^{n+2} + a^{n+1} - 1 = 0$ in $(0, 1)$. We conclude that if $a \in (a_{2n+3,L}, \bar{a}_{2n+3})$, inequality (C.4) holds.

Next, we examine Eq.(C.3). Let

$$\varphi_1(b) = \log \frac{1-a}{1-b} \quad \text{and} \quad \hat{\varphi}_2(b) = \frac{(b-a)(1+ab^n)\Sigma_{k=0}^n b^k}{a^2 b^{2n+1}}.$$

Clearly, $\varphi_1(a) = \varphi_2(a)$. We can easily see that $\varphi_1(b)$ is a monotonically increasing convex function and $\lim_{b=1} \varphi_1(b) = \infty$. Moreover, we have

$$\varphi_2(1) = \frac{(n+1)(1-a^2)}{a^2} \quad \text{is bounded for } a \in (0, 1) \text{ and}$$

$$\frac{d\varphi_2(a)}{db} = \frac{\Sigma_{k=0}^{2n+1} a^k}{a^{2n+3}} > 0.$$

Therefore, if

$$\frac{d\varphi_1(a)}{db} = \frac{1}{1-a} < \frac{\Sigma_{k=0}^{2n+1} a^k}{a^{2n+3}} \Rightarrow a^{2n+3} + a^{2n+2} - 1 < 0,$$

$\varphi_1(b)$ intersects $\hat{\varphi}_2(b)$ at least one point $b \in (a, 1)$. Let $\hat{a}_{2n+3}$ be a root of the equation $a^{2n+3} + a^{2n+2} - 1 = 0$ in $(0, 1)$. We conclude that if $a < \hat{a}_{2n+3}$, there exists $b \in (a, 1)$ such that, for a and b, Eq.(27) holds. Let $a_{2n+3,R} = \min\{\bar{a}_{2n+3}, \hat{a}_{2n+3}\}$. Now, we can state that if $a \in (a_{2n+3,L}, a_{2n+3,R})$, there exists $b \in (a, 1)$ and $\beta > 0$ such that for (a, b, β), we have a period-$2n + 3$ Markov partition of the unit interval with respect to f.

Finally, we show that f is eventually expanding. Let I_k $(k = 1, 2, \ldots n - 1)$ be subintervals of the period-$2n + 3$ Markov partition and $I^* = [\theta_L, \theta_R]$. Moreover, let $\bar{I}_k$ be an interior of I_k. A minor consideration shows that every point $x \in \bigcup_{k=1}^{k} \bar{I}_k$ will visit I^* at least once every $2n + 2$th iteration. Therefore, for $x \in \bigcup_{k=1}^{k} \bar{I}_k$,

$$\left| (f^{2n+2})'(x) \right| \geq a^{2n+1} |\phi'| \geq \left| -\frac{a^{2n+3}}{1 - a} \right|,$$

and if

$$\left| -\frac{a^{2n+3}}{1 - a} \right| > 1 \Rightarrow a^{2n+3} + a - 1 > 0, \tag{C.7}$$

map f is eventually expanding. We can easily see that if $a_{2n+3,L} < a$, inequality (C.7) holds. This completes the proof. □

References

[1] Asano, T., Kunieda, T., and Shibata, A., 2012. Complex Behaviour in a Piecewise Linear Dynamic Macroeconomic Model with Endogenous Discontinuity. Journal of Difference Equations and Applications 18, 1889-1898.

[2] Asano, T., Yokoo, M., 2019. Chaotic Dynamics of a Piecewise Linear Model of Credit Cycles. Journal of Mathematical Economics 80, 9-21.

[3] Benhabib, J., Day, R.H., 1982. A Characterization of Erratic Dynamics in the Overlapping Generations Model. Journal of Economic Dynamics and Control 4, 37-55.

[4] Boyarsky, A., Góra, P., 1997. Laws of Chaos: Invariant Measures and Dynamical Systems in One Dimension, Springer.

[5] Gardini, L., Sushko, I., and Naimzada A. K., 2008. Growing through Chaotic Intervals. Journal of Economic Theory 143, 541-557.

[6] Grandmont, J., 1985. On Endogenous Competitive Business Cycles. Econometrica 53, 995-1045.

[7] Hata, M., 2014. Neurons: A Mathematical Ignition. Singapore: World Scientific Publishing.

[8] Ishida, J., Yokoo, M., 2004. Threshold Nolinearities and Asymmetric Endogenous Business Cycles. Journal of Economic Behavior and Organization 54, 175-189.

[9] Iwaisako, T., 2002. Technology Choice and Patterns of Growth in an Overlapping Generations Model. Journal of Macroeconomics 24, 211-231.

[10] Matsuyama, K., 2007. Credit Traps and Credit Cycles. American Economic Review 97, 503-516.

[11] Matsuyama, K., 2013. The Good, the Bad, and the Ugly: An Inquiry into the Causes and Nature of Credit Cycles. Theoretical Economics 8, 623-651.

[12] Matsuyama, K., Sushko, I., and Gardini, I., 2016. Revisiting the Model of Credit Cycles with Good and Bad Projects. Journal of Economic Theory 163, 525-556.

[13] Nagumo, J., Sato, S., 1972. On a Response Characteristic of a Mathematical Neuron Model. Kybernetik 10, 155-164.

[14] Nusse, H. E., Yorke, J. A., 1995. Border-Collision Bifurcation for Piecewise Smooth One-Dimentional Maps. Journal of Bifurcation and Chaos 5, No.1, 189-207.

[15] Sushko, I., Avrutin, V., and Gardini, L., 2015. Bifurcation Structure in the Skew Tent Map and Its Application As a Border Collision Normal Form, Journal of Difference Equations and Applications 21, 1-48.

[16] Umezuki, Y., Yokoo, M., 2019. A Simple Model of Growth Cycles with Technology Choice. Journal of Economic Dynamics and Control 100, 164-175.

[17] Yokoo, M., Ishida, J., 2008. Misperception-Driven Chaos: Theory and Policy Implications. Journal of Economic Dynamics and Control 32, 1732-1753.

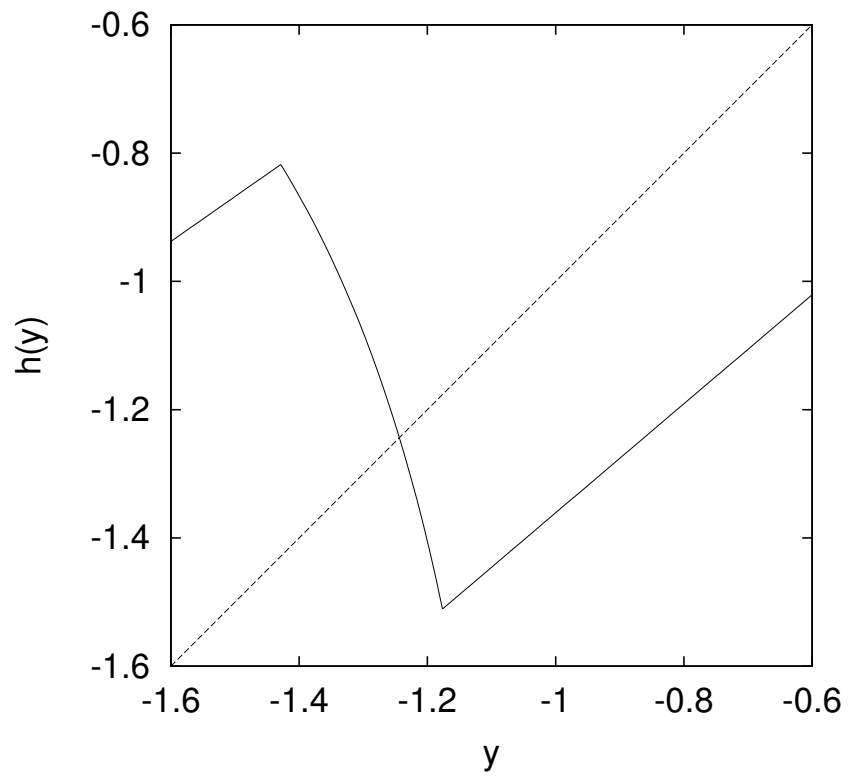Figure 1: Piecewise smooth map (17) which has the fixed point in $\left(-\frac{1}{a}, -\frac{1}{b}\right)$. $a = 0.7, b = 0.85$ and $\beta = 4$.
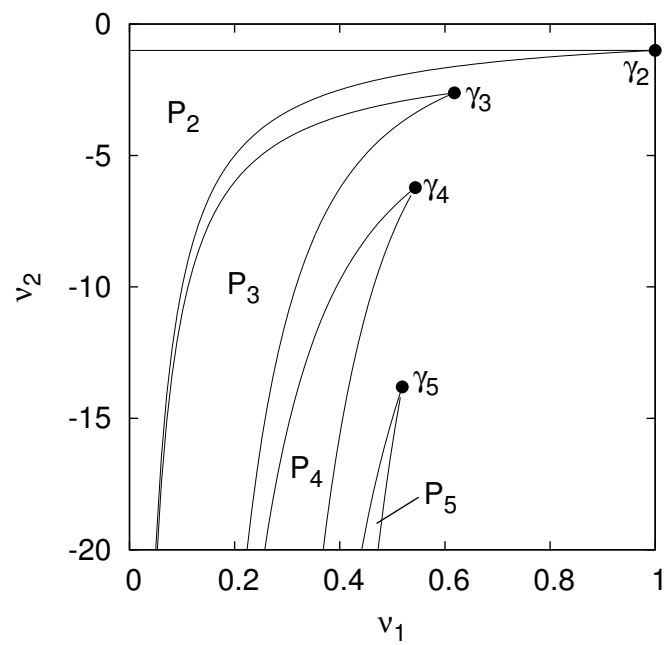
Figure 2: The sets P_2, P_3, P_4 and P_5 on the (ν_1, ν_2)-plane. If $(\nu_1, \nu_2) \in P_k$, the map (18) has an attracting period-k cycle.
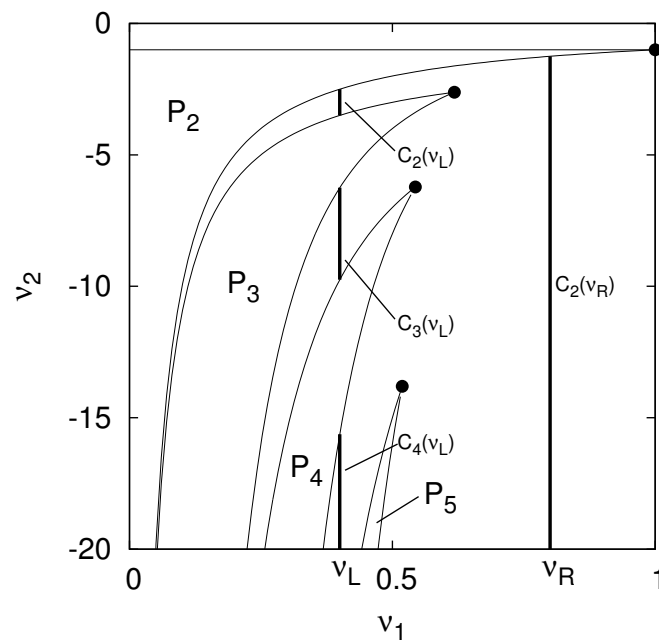
Figure 3: Some examples of the set C_m on the (ν_1, ν_2)-plane. The sets $C_2(\nu_L), C_3(\nu_L)$ and $C_4(\nu_L)$ are bounded, while the set $C_2(\nu_R)$ is unbounded. Note that $L(\nu_R) = C_2(\nu_R)$ and $L(\nu_L) = C_2(\nu_L) \cup C_3(\nu_L) \cup C_4(\nu_L) \cup \dots$.
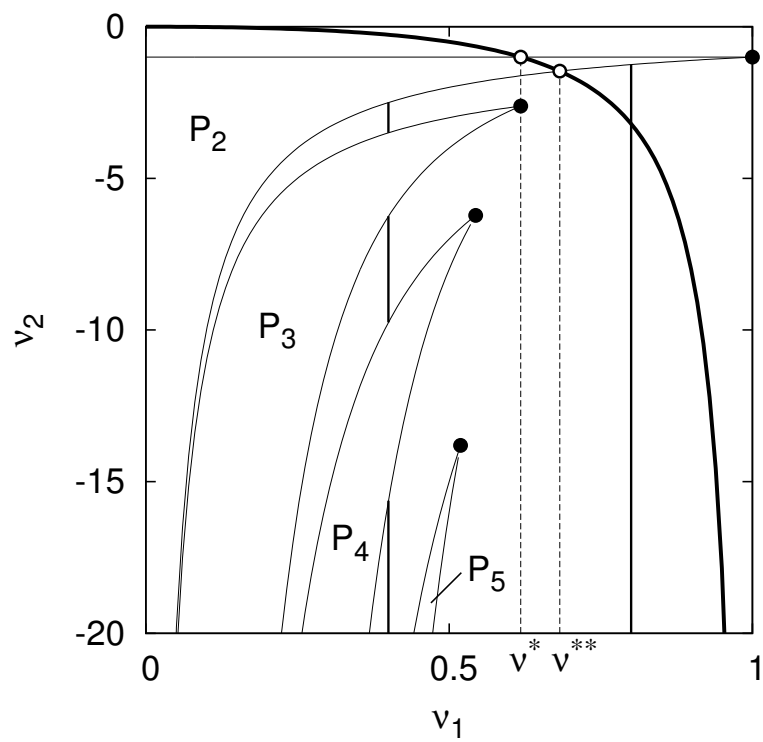
Figure 4: The line $\nu_2 = -\frac{\nu_1^2}{1-\nu_1}$ on the $(\nu_1 \nu_2)$-plane. For $a > \nu^{**}$, our model has the capability to generate chaotic dynamics induced by border collision bifurcation.
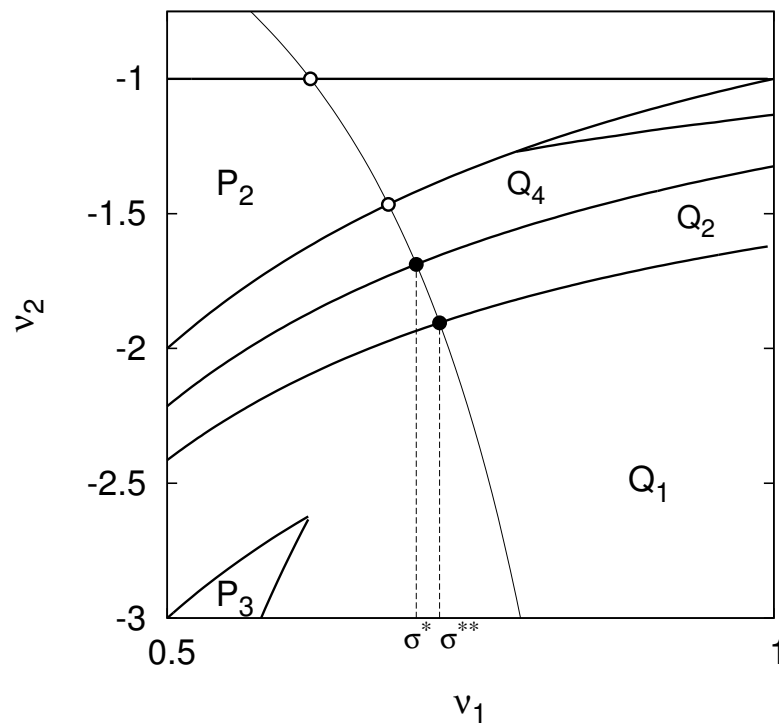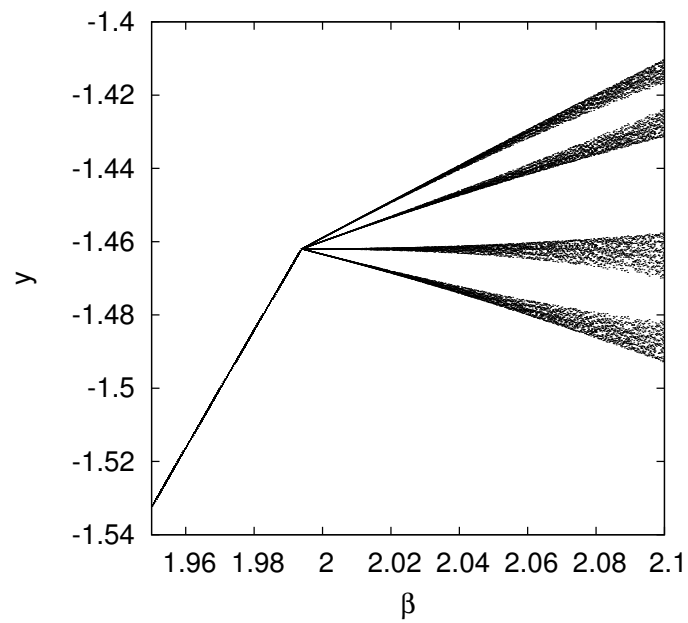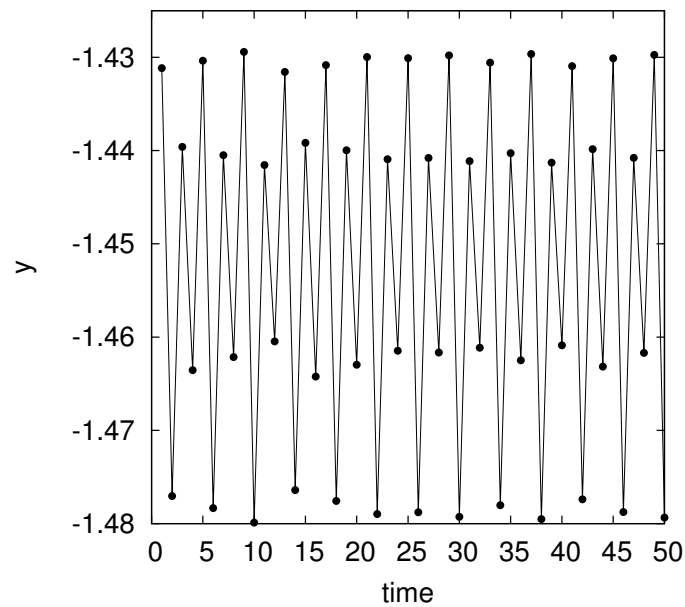
Figure 5: Classification of the chaotic region. Depending the value *a*, our model exhibit four-piece, two-piece and one-piece chaotic attractor which relate to the region Q_4, Q_2 and Q_1, respectively.

(a) Bifurcation diagram of map (20) with respect to β..

(b) Time series obtained from map (20) with four-piece chaotic attractor.

Figure 6: Panel (a) depicts the bifurcation diagram of map (20) respect to β, where $a = 0.684 \in (\nu^{**}, \sigma^*)$. Panel (b) depicts time series obtained from map (20) with $a = 0.684$ and $\beta = 2.06$.
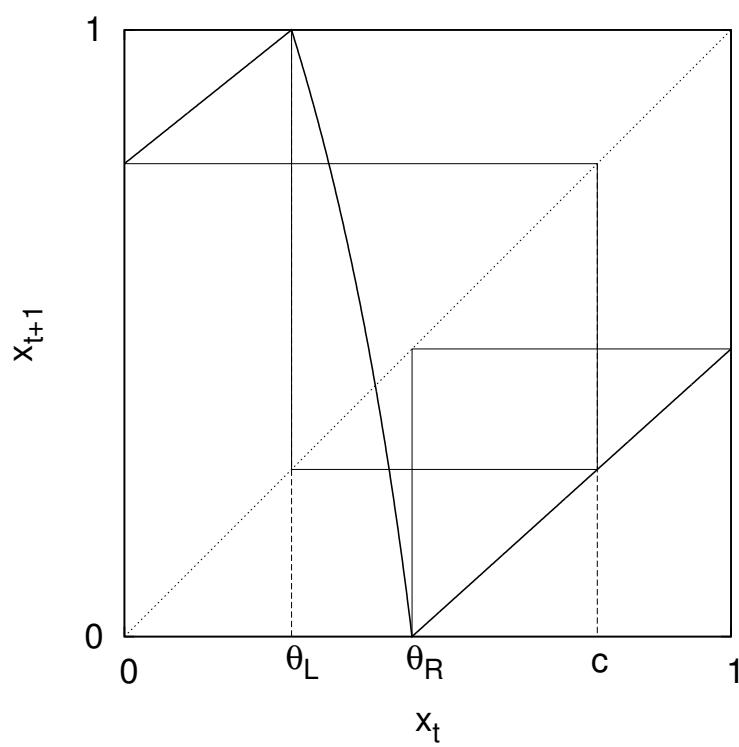
Figure 7: The map (24) with a period-5 Markov parition. $a = 0.8, b \approx 0.902$ and $\beta \approx 6.507$.